ISSN 1027-4510, Journal of Surface Investigation. X-ray, Synchrotron and Neutron Techniques, 2009, Vol. 3, No. 3, pp. 429–436. © Pleiades Publishing, Ltd., 2009.
Original Russian Text © V.T. Lebedev, 2009, published in Poverkhnost'. Rentgenovskie, Sinkhrotronnye i Neitronnye Issledovaniya, No. 6, pp. 14–21.

# Principles of Generalized Spin-Echo Spectroscopy

**V. T. Lebedev**

*Konstantinov St. Petersburg Institute for Nuclear Physics, Russian Academy of Sciences, Orlova roshcha 1, Leningrad Oblast, Gatchina, 188300 Russia*

*e-mail: vlebedev@pnpi.spb.ru*

Received January 20, 2008

**Abstract**—The concept is proposed for determining the total dynamic scattering function of an object under study, representing a sum of odd and even parts measured by the generalized neutron spin-echo method in the form of the signals $S_{odd}(q, t) \sim \int S(\omega, q)\sin(\omega t)d\omega$ and $S_{even}(q, t) \sim \int S(\omega, q)\cos(\omega t)d\omega$ as functions of the momentum $q$ transferred to the neutron and the time $t$ corresponding to the frequency $\omega$ and the transferred energy $\hbar\omega$. The principle of the generalized spin echo and the results of mathematical modeling are confirmed in experiments on inelastic scattering on magnetic fluids and polymer solutions. The developed method makes it possible to study the features of the dynamics of atomic and molecular systems, e.g., to analyze soft vibrational spectra of nanoparticle ensembles against the background of intense relaxation processes, which is inaccessible for classical spin-echo spectrometry.

**DOI:** 10.1134/S1027451009030161

## INTRODUCTION

The neutron spin echo (NSE) [1, 2] is the most precise method for studying matter dynamics in the energy range of low-frequency excitations (phonons, magnons, diffusion and relaxation modes, and others), which spans more than six orders of magnitude, $\hbar\omega = 10^{-10}$–$10^{-3}$ eV [3], beginning from extremely low energies below the nanoelectronvolt region, whose measurement is inaccessible for other neutron methods [4, 5]. The modernization of the classical NSE, proposed in [1, 2], by modulating the primary neutron spectrum in wavelengths by a phase of the Larmor precession of the neutron spin in a magnetic field provides independent analysis of changes in the neutron velocity and spin state during the interaction with a sample. This makes it possible to study matter dynamics in strong magnetic fields in combination with three-dimensional analysis of scattered neutron polarization [6, 7], independently obtaining information on the behavior of nuclear and magnetic subsystems of a sample in the range of atomic and molecular time scales $10^{-13}$–$10^{-7}$ s [5]. A characteristic feature of the NSE method, in contrast to classical neutron spectroscopy operating in the frequency–momentum coordinates $(\omega, q)$, is the measurement of the scattering function $S(t, q)$ of an object in the time–momentum space, which gives certain advantages in the study of relaxation processes in molecular systems (polymers) and analysis of anharmonicity phenomena in atomic and molecular vibrations. The most efficient analysis of matter dynamics is achieved when combining the classical time-of-flight technique of inelastic neutron scattering [8] or triaxial crystal-diffraction tools [9, 10] and the spin-echo method which makes it possible to measure the frequency spectrum and to determine the excitation lifetimes from a data set in the $(\omega, q)$- and $(t, q)$-space in a single experiment.

In addition to the above achievements, we note that the cosine of the Fourier transform of the scattering function is always determined in spin-echo spectrometry studies. The signal is measured, which characterizes only the even frequency component $S_{even}(q, t) \sim \int S(\omega, q)\cos(\omega t)d\omega$ of the total scattering function $S(\omega, q) = S_{odd}(\omega, q) + S_{even}(\omega, q)$, where $S_{odd}(\omega, q) = [S(\omega, q) - S(-\omega, q)]/2$, $S_{even}(\omega, q) = [S(\omega, q) + S(-\omega, q)]/2$. Such NSE experiments provide real insight into the dynamics of systems whose scattering function is even with sufficient accuracy. For fundamental reasons, asymmetry always exists in the scattering function. According to the detailed balance principle, the equality $S(-q, -\omega) = \exp(-\hbar\omega/kT)S(q, \omega)$ is satisfied, which reflects the fact that transitions from low-energy levels to high-energy levels are more probable than reverse ones (the level population according to Boltzmann) [11]. In the case of equilibrium systems at low excitation energies, $\hbar\omega/kT \ll 1$, which can also be analyzed using classical NSE experiments, we can neglect the contribution of odd effects to the total scattering function. The time behavior of nonequilibrium (metastable) systems, as shown below, is significantly controlled by odd dynamic effects (polymers, ferromagnetic fluids).

As for the time behavior of dynamic systems, we note that the time scattering function is even for reversible deterministic processes, $S(t, \mathbf{q}) = S(-t, \mathbf{q})$ (e.g., oscillations of the classical oscillator without damping). In

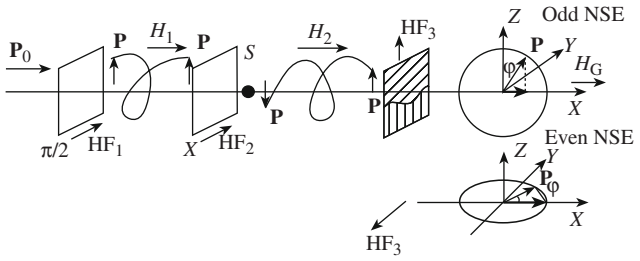


**Fig. 1.** Experimental scheme of the odd and even spin-echo method (top, bottom). The evolution of the polarization vector $\mathbf{P}_0 \longrightarrow \mathbf{P}$ as the neutron passes through π/2- and π flippers (fields $HF_{1,2,3}$, flipper coils are shown) and fields $H_{1,2}$. Neutron scattering from the sample *S* does not cause polarization change.

stochastic processes, the parity is violated. For example, if a system evolves to a critical state in the form of a set of metastable states transforming into each other by means of "avalanches" caused by a local external perturbation (self-organized criticality) [12]. Odd effects were detected in spin dynamics, i.e., three-spin correlations during second-order phase transitions [13, 14] and chiral scattering in magnets [15]. High-order correlations and associated odd effects in dynamics are possible in polymers near the θ-point [16], when pair interactions of units spaced along the chain disappear [16]. The existence of the $S(q, \omega)$ asymmetry is obvious during the interaction of ultracold neutrons with matter, in neutron optics of moving boundaries (phase space transformers), during neutron scattering in the ground-state or strongly excited systems. In view of the importance and diversity of the dynamics problems associated with the parity violation of the frequency and time scattering functions, the generalized neutron spin-echo method was developed for analyzing odd and even components of the dynamic scattering function of objects under study [17].

## 2. PRINCIPLES OF MEASURING ODD AND EVEN COMPONENTS OF THE SCATTERING FUNCTION

Figure 1 shows the scheme of the neutron spin-echo experiment for measuring odd and even scattering functions of an object. The monochromatized polarized beam of polarized neutrons (the wavelength spectrum is $W(\lambda)$, the width is $\Delta\lambda/\lambda \ll 1$, and the initial polarization vector is $\mathbf{P}_0$) sequentially passes through the regions of magnetic fields $H_1$ and $H_2$, in which Larmor precession of the neutron polarization vector occurs. The precession regions are partitioned by a device for rotating the polarization vector by the angle π (π flipper), and the input and output boundaries of the regions are bounded by flippers rotating the neutron polarization by the angle π/2. At the output of the 2nd precession field, the neutron polarization gains the phase $\varphi = \gamma_L(L_1H_1/v_1 - L_2H_2/v_2)$, where $L_1$ and $L_2$ are field lengths, $\gamma_L$ is the gyromagnetic ratio, and $v_1$ and $v_2$ are neutron velocities in the precession regions $H_{1,2}$ (Fig. 1) [2]. In the case of equal field integrals ($L_1H_1 = L_2H_2$) and elastic scattering ($v_1 = v_2$), the phase $\varphi = 0$ in the entire neutron spectrum and the resulting vector of beam polarization is $\mathbf{P} = \mathbf{P}_0$. The polarization is completely restored after precession in fields, which is called the spin-echo focusing effect. If the neutron velocity changes after scattering ($v_1 \neq v_2$, inelastic process), at equal field integrals, the polarization vector of the neutrons of a certain wavelength has two components $P_Y/P_0 = \sin(\varphi)$ and $P_Z/P_0 = \cos(\varphi)$, which depend on the phase that is exactly the measure of the neutron energy (velocity and wavelength) change.

In the standard NSE configuration, flippers are installed in parallel positions. The *Z*-projection of the polarization vector integrated over the spectrum is measured. According to the spin-echo theory [1], this projection is the Fourier transform $S_{even}(\mathbf{q}, t) \sim \int S_{even}(\omega, \mathbf{q})\cos(\omega t)\, d\omega$ of the even part of the scattering function depending on the time $t = \hbar\pi N/E_0$, where *N* is the number of precessions in each field region for neutrons with the spectrum-averaged energy $E_0$. In these experiments, the *Y*-component reflecting the odd part $S_{odd}(\omega, \mathbf{q})$ of the total spectrum $S(\omega, \mathbf{q})$ is ignored. To reconstruct $S_{odd}$, an orthogonal configuration of flippers was proposed [1] (Fig. 1), which allows measurement of the Fourier transform of the odd component $S_{odd}(\mathbf{q}, t) \sim \int S_{odd}(\omega, \mathbf{q})\sin(\omega t)\, d\omega$. In the case of elastic scattering, the zero signal is measured in this configuration.

Thus, both components $S_{even}(\mathbf{q}, t)$ and $S_{odd}(\mathbf{q}, t)$ can be measured by installing the parallel and orthogonal flipper positions. It should be emphasized that there is no way to strictly separate the components in conventional spectroscopy in the coordinates $(\omega, \mathbf{q})$, and the odd part is masked by the even part.

To illustrate the capability of the generalized spin-echo method, model signals were constructed (Fig. 2). Such frequency spectra are observed, in particular, for three-spin correlations [14] (odd part) mixed with pair correlations (spin diffusion),

$$S_{even} = (1/\pi)[1 + (\omega\tau)^2]^{-1},$$

$$S_{odd} = (\varepsilon/\pi)(\omega\tau)/[1 + (\omega\tau)^2]^2,$$

where τ defines the linewidth $\hbar/\tau$, the parameter $\varepsilon = 1.54$ was chosen from the condition $S_{oddMAX} = (1/2)S_{evenMAX}$, and the coefficient $(1/\pi)$ provides the normalization $\int S_{even}(\omega\tau)d(\omega\tau) = 1$. Spin-echo signals (Fourier transforms) corresponding to these spectra are given by

$$S_{even}(t/\tau) = \exp(-t/\tau);$$

$$S_{odd}(t/\tau) = (\varepsilon/2)(t/\tau)/\exp(-t/\tau).$$

As Fig. 2a shows, it is difficult to conclude on the presence of the odd component immediately from the general spectrum $S(\omega) = S_{even} + S_{odd}$, even if it reaches half the even signal amplitude. In the spin-echo representation,

the components are separated (Fig. 2b), and the odd part $S_{odd}(t/\tau) \geq S_{even}(t/\tau)$ dominates for times $t \geq 1.5\tau$. The features of the odd dynamics are considered below by the example of ferromagnetic fluids and polymer solutions.

## 3. DYNAMICS OF FERROMAGNETIC FLUIDS AND POLYMERS

The generalized spin-echo method was tested in experiments with the "MESS" NSE spectrometer (Leon Brillouin Laboratory, Saclay, France). An output $\pi/2$ flipper was installed in parallel and orthogonal positions. Inelastic scattering was measured in two different molecular systems.

Ferromagnetic fluid (FF) [18] with 18 vol % of $Fe_3O_4$ particles (of diameter $D_m \sim 10$ nm) stabilized in pentanol by a surfactant (a bilayer ~3 nm thick of oleic and dodecyl benzene sulfonic acids) was used as the first sample. In a high-density ($d = 1.69$ g/cm$^3$) FF with saturation magnetization ($4\pi M_S = 860$ G), the particles covered by shells (outer diameter $D_P \sim 16$ nm) were at a distance of ~20 nm comparable to their size that caused strong magnetic and molecular interactions of particles and odd effects in dynamics.

The second sample was a heavy-water solution of poly-(*N*-vinyl caprolactam) (PVCL) with the mass $M = 1 \times 10^6$ and gyration radius $R_G \sim 40$ nm. The polymer concentration $c = 1.4$ g/dl was chosen above the PVCL coil overlap threshold ($C^* \sim 0.5$ g/dl) to observe mostly their internal (segmental) dynamics at temperatures $T < T_\theta$ close to the Flory θ-temperature $T_\theta = 32°C$. Above it, the coil–globule transition is observed [19]. At the point $T = T_\theta$, pair interactions of units mutually spaced in the chain disappear, and higher-order interactions dominate, at which odd effects in polymer dynamics can be expected.

In NSE experiments, an echo-group was measured by 12 points; the data were calibrated by their normalizing to the signal of an elastic scatterer (graphite). The intensities $I^{\pm} = (1/2)\int [1 \pm P]\, I_T d\lambda d\omega$ of scattered neutrons with spins along and opposite to the guiding field depend on the sum of components $I_T(\lambda, \omega) = I^+ + I^-$ and the polarization $P(\lambda, \omega) = (I^+ - I)/(I^+ + I^-)$.

To obtain information on sample dynamics, it is sufficient to determine only one component, e.g., $I^+(t, h) \sim \int W(\lambda)d\lambda \int S(\omega, q)d\omega + \int W(\lambda)d\lambda \int S(\omega, q)P[\omega t, \psi]d\omega$, where $W(\lambda)$ is the spectrum of the primary beam wavelength, $P = P_0 \cos(\omega t + \psi)$ and $P = P_0 \sin(\omega t + \psi)$ in the even and odd modes. The phase $\psi = \psi_0(\lambda/\lambda_0) \sim \lambda h$ depends on the wavelength and the difference $h(i)$ of spectrometer shoulder fields, proportional to the correcting coil current $i$ in measuring the echo group (Fig. 3). The phase $\psi_0 = \psi$ corresponds to the central wavelength $\lambda = \lambda_0$ in the spectrum. In the case of a narrow symmetric

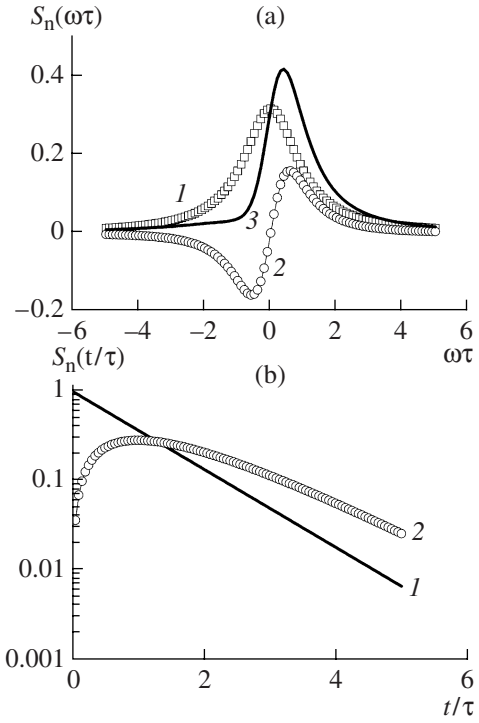


**Fig. 2.** Modeling of the frequency spectra and spin-echo time signals: (a) even, odd, and total frequency functions (curves *1*, *2*, *3*) and (b) NSE signals (curves *1*, *2*) of functions *1*, *2* (a).

spectrum ($\Delta\lambda/\lambda_0 \sim 0.1$), the measured intensities are given by

$$\begin{aligned} I^+(t, \psi_0)_{even} &= A_0 + A_P S_{even}(t)\cos\psi_0 \\ &\quad - A_P S_{odd}(t)\sin\psi_0, \\ I^+(t, \psi_0)_{odd} &= A_0 + A_P S_{even}(t)\sin\psi_0 \\ &\quad + A_P S_{odd}(t)\cos\psi_0, \end{aligned} \tag{1}$$

where $A_0 \sim \int W(\lambda)d\lambda \int S(\omega, q)d\omega = \text{const}$ is the total scattering intensity. The parameter $A_P \sim \int P_0(\lambda)W(\lambda)d\lambda$ is constant in an ideal NSE; in practical experiments, $A_P(t)$ is the function of time due to a focusing violation under strong precession fields. For an elastic scatterer, equalities (1) become simpler,

$$I^+(t, \psi_0)_{even0} = A_{0el} + A_{PEL}(t)\cos\psi_0,$$

$$I^+(t, \psi_0)_{odd0} = A_{0el} + A_{PEL}(t)\sin\psi_0.$$

In the experiments, the amplitudes $A_{PEL}(t)$ were determined at each value of the spin-echo time *t,* by approximating the curves $I^+(t, \psi_0)_{even0}$ and $I^+(t, \psi_0)_{odd0}$ by harmonic functions. The data for samples were approximated in a similar way and the functions $A_{even} = A_P(t)S_{even}(t)$, and $A_{odd} = A_P(t)S_{odd}(t)$ were determined,

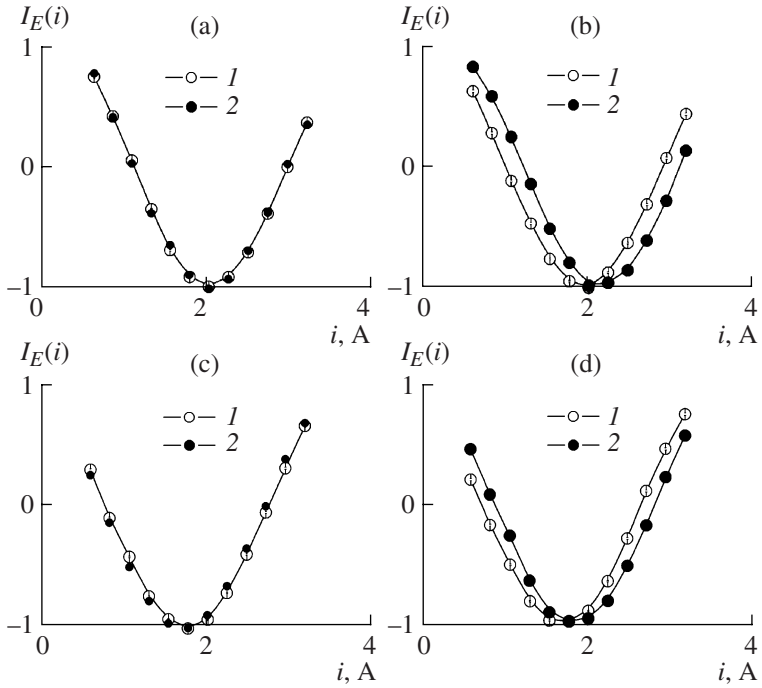


**Fig. 3.** Echo groups (*1*, *2*) for graphite and ferromagnetic fluid (20°C, the scattering angle is θ = 1.7°) in parallel and crossed positions (a, b; c, d): (a, c) the NSE time is $t = 0.25$ and 0.5 ns (the data are averaged); (b, d) the time is $t = 10$ ns. The intensities, i.e., the functions of the correcting coil current $I_E(i) = [I(i) - A_0]/A_{EFF}$, are reduced to the effective amplitude $A_{EFF}$ after subtracting the average $A_0$. Curves are approximating functions (*1*).

which were normalized to the "elastic" amplitude $A_P(t)$ to find the sought signals $S_{even}(t)$ and $S_{odd}(t)$.

The method for determining the scattering functions $S_{even}(t)$ and $S_{odd}(t)$ can also be used, in which the intensities $I^{\pm}(t, \psi_0)_{even}$ and $I^{\pm}(t, \psi_0)_{odd}$ are measured for the sample and elastic scatterer, from which the polarization and spin-echo signals are determined,

$$P_{even}(t) = a_{ev}(t)\cos\psi_0 - a_{od}(t)\sin\psi_0;$$
$$P_{odd}(t) = a_{ev}(t)\sin\psi_0 + a_{od}(t)\cos\psi_0;$$

$$P_{oev}(t) = a_0(t)\cos\psi_0; \quad P_{ood}(t) = a_0(t)\sin\psi_0;$$

$$S_{even}(t) = a_{ev}(t)/a_0(t) = [P_{even}(t)P_{oev}(t) + P_{odd}(t)P_{ood}(t)]/[P_{oev}(t)^2 + P_{ood}(t)^2];$$

$$S_{odd}(t) = a_{od}(t)/a_0(t) = [P_{odd}(t)P_{oev}(t) - P_{even}(t)P_{ood}(t)]/[P_{oev}(t)^2 + P_{ood}(t)^2].$$

The feature of the developed approach is the consideration of the signal phase shift due to odd effects. But if only the amplitude of the spin-echo signal is extracted from the $I^{+}(t, \psi_0)_{even}$ data as in conventional spin-echo spectrometry, it is becomes clear that the amplitude $A(t)_{EFF} = A_P[S^2_{even} + S^2_{odd}]^{1/2} \approx A_P S_{even}[1 + (1/2)(S_{odd}/S_{even})^2]$ contains the contribution of the odd effect $\Delta S_{even}/S_{even} \approx (1/2)(S_{odd}/S_{even})^2$. At $S_{odd}/S_{even} \le 10\%$, the correction $\Delta S_{even}/S_{even} \le 0.5\%$ is small and can be ignored. However, at $S_{odd}/S_{even} \ge 50\%$, the distortions $\Delta S_{even}/S_{even} \ge 10\%$ become significant. To confirm this, the results on FF and polymer dynamics in the solution were obtained based on Eq. (1).

Figure 3 compares the echo groups for FF and graphite, measured at 20°C and the scattering angle θ = 1.7° at times $t = 0.25$, 0.5, and 10 ns in the cases of parallel and crossed flipper positions. The echo-group phase shift increases to 20° with the time $t$, hence, neutrons transfer energy to the system (excited states are less probable than low-energy states), although the neutron temperature ($T_N \sim 20$ K) is ten times lower than the sample temperature ($T = 293$ K).

The even functions measured in parallel and crossed flipper configurations have close values (Fig. 4). The odd scattering functions obtained in the same experiments diverge, which indicates that the FF state changed between measurements, approaching the equilibrium for a day. The data obtained by the odd spin-echo method show nonequilibrium dynamics inherent to the ferromagnetic fluid as a metastable system with macroscopic (structural, magnetic) relaxation times. Slow relaxation (~$10^4$ s) in these FFs was previously observed using small-angle neutron scattering [18].

The function $S_{even}(t)$ characterizing the even effects is quasistatic at momenta $q = 0.31$, 0.55, and 0.91 nm$^{-1}$ in the time range $t = 0.1$–10 ns (Fig. 5). The $S_{even}(t)$ damping becomes appreciable only at $t > t^* \sim 10$ ns. The momenta $q > 1/D_P$ are larger than the inverse particle size. Therefore, autocorrelations dominate in the dynamics, which are described in the Gaussian approx-

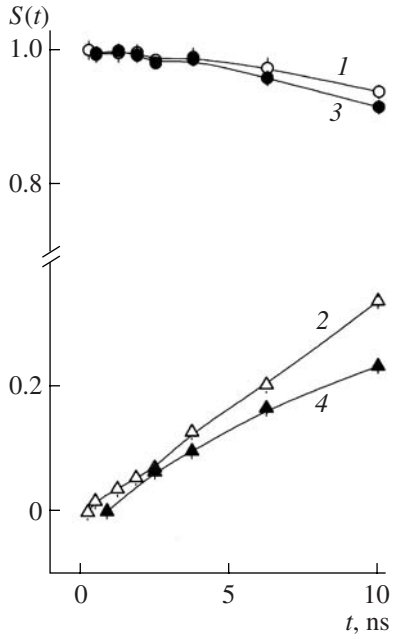


**Fig. 4.** Spin echo in (*1*, *2*) parallel and (*3*, *4*) crossed positions for (*1*, *3*) even and (*2*, *4*) odd scattering functions of ferromagnetic fluid at 20°C; the scattering angle is θ = 1.7°.

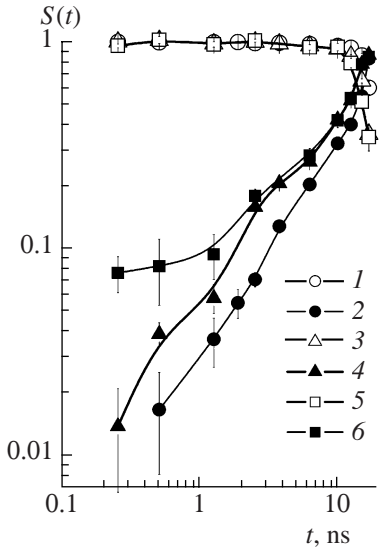


**Fig. 5.** (*1*, *3*, *5*) Even and (*2*, *4*, *6*) odd components of the dynamic scattering function of ferromagnetic fluid at 20°C and momenta $q$ = (*1*, *2*) 0.31; (*3*, *4*) 0.55, and (*5*, *6*) 0.91 nm$^{-1}$. Curves are spline functions.

imation as $S_{even}(t) \sim \exp[-q^2\Gamma(t)/2]$, where $\Gamma(t)$ is the squared particle displacement for the time $t$. Diffusion of individual particles with a delay for the induction time $t^* \sim 10$ ns is observed, which is explained by the "cage effect", when the particle motion is associated with regrouping of neighboring particles.

In contrast to even correlations, the odd part increases approximately linearly in the entire time range. The rate of its increase depends on the momentum, which is especially appreciable at short times, $t \le 1$ ns. At $t > 10$ ns, the curves for different momenta converge (Fig. 5). Features of odd dynamics become distinct when the function $S_{odd}(t)$ is normalized to the time (Fig. 6). The functions $S_{odd}(t)/t$ show oscillations in time, which mean that neutrons excite particle oscillations during scattering, which are described by the function $S_{odd}(t)/t = F(t) = \langle\omega\rangle + \beta t^2 + \mu\cos(\Omega t)\exp(-\nu t)$ with the parameters given in the table. The odd dynamics (Fig. 6) is different at momenta $q_1 = 0.31$ , $q_2 = 0.55$, and $q_3 = 0.91$ nm$^{-1}$. The value of $q_1 \sim \pi/D_m$ is close to the maximum possible acoustic wave momentum in the chain of bound particles, the distance between centers is equal to the magnetic core diameter $D_m \sim 10$ nm. Excitation of such a mode with frequency $\Omega \sim 0.5$ rad/ns in a concentrated particle system seems to be quite feasible. Modes with frequency $\Omega \sim 0.3$ rad/ns at $q_2$ and $q_3$ should be attributed to oscillations of individual particles with a period $T_\Omega \sim 20$ ns and decay time $\tau = 1/\nu \sim T_\Omega/2 \sim 10$ ns. In addition to rapid oscillations, a slow mode was detected at the frequency $\langle\omega\rangle = [\int \omega S(\omega, \mathbf{q})d\omega]/[\int S(\omega, \mathbf{q})d\omega] \sim (3\text{–}5) \times 10^7$ rad/s. At the momentum $q_1$, its period is $T_{q1} = 2\pi/\langle\omega\rangle \sim 200$ ns. At $q_2$ and $q_3$, the mode period $T_{q23} \sim 100$ ns is twice smaller, but is outside the experimental range $t$ = 0–20 ns. The frequency $\langle\omega\rangle$ increases with the momentum, and the ratio $\langle\omega\rangle/q \sim U \sim 10$ cm/s characterizes the excitation propagation velocity which appears smaller than the speed of sound in molecular liquids by four orders of magnitude. The ratio oscillations–slow component

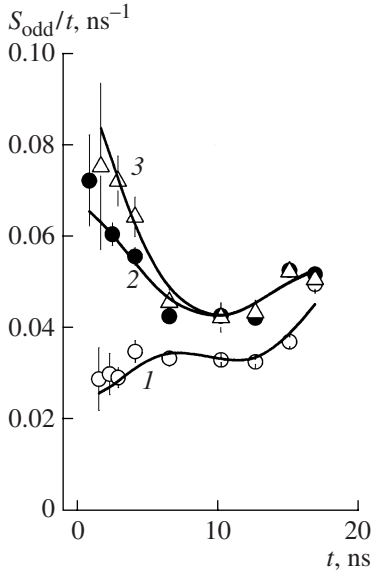


**Fig. 6.** Odd dynamics: the function $S_{odd}(t)/t$ at $q$ = 0.31, 0.55, and 0.91 nm$^{-1}$ (*1*–*3*). Curves are fitting functions $F(t)$.

Parameters of the odd scattering function

| $q$, nm$^{-1}$ | $\langle\omega\rangle$, $10^7$ s$^{-1}$ | $\beta$, 1/ns$^3$ | $\mu$,$10^7$ s$^{-1}$ | $\Omega$, $10^9$ s$^{-1}$ | $\nu$, $10^9$ s$^{-1}$ |
|---|---|---|---|---|---|
| 0.31 | 2.9 ± 0.2 | (5 ± 1)$10^{-5}$ | –0.44 ± 0.11 | 0.50 ± 0.02 | – |
| 0.55 | 4.9 ± 0.2 | – | 1.7 ± 1.0 | 0.32 ± 0.02 | 0.072 ± 0.062 |
| 0.91 | 5.1 ± 0.1 | – | 4.2 ± 1.1 | 0.30 ± 0.02 | 0.14 ± 0.04 |

$\mu/\alpha \sim$ 15–80% changes in favor of oscillations as the momentum increases. On the particle radius scale $D_m/2 \sim 2\pi/q_3$, the contributions of rapid and slow components are comparable. At a small momentum, odd correlations are enhanced with delay $t^* \sim 10$ ns, which is taken into account by adding the term $\beta t^2$ to the function $F(t)$. It is of interest to compare the data for even and odd parts of the scattering function.

The time dependence of the even part $S(t)_{\text{even}} = \exp[-q^2\Gamma(t)/2]$allows us to determine how the particle moves. Its displacement $\Delta X = \Gamma(t)^{1/2} = [-(2/q^2)\ln(S)]^{1/2}$ increases to $\Delta X(t) \sim 1$ nm at times $t <$ 15 ns, and then it jumps to the value $\Delta X \sim 3$ nm of the order of the particle core radius (Fig. 7). At $t < 15$ ns, the time dependence of the displacement is described by the function $\Delta X(t) = [a^2 + (vt)^2]^{1/2}$, where $a$ = 0.4 ± 0.1 nm is the amplitude of rapid oscillations, $v$ = 8.7± 0.3 cm/s is the particle velocity component along **q** (data for $q_1$). Oscillating with small amplitude, the particle slowly drifts until conditions arise for a jump to a distance of the order of the core radius. The velocity $v$ = 8.7 cm/s is ten times lower than the particle thermal velocity $V_T = (kT/m_P)^{1/2} \sim 100$ cm/s ($m_P$ is the particle mass). The moving particle entrains solvent and neighbors, affecting two coordination spheres (i.e., a volume ~100 times larger than the particle volume). Comparing even and odd dynamics, we can see that the time of particle oscillation damping $\tau = 1/\nu \sim T_\Omega/2 \sim 10$ ns is comparable with the induction period, after which the particle breaks from a "cage" to a new position. Observation of even effects makes the impression that the particle motion is reduced to "jitter" and drift and jump to a new position (diffusion in liquids). The odd effects show a missing "stage", i.e., soft modes, oscillations without which jumps are impossible. The odd dynamics provides insight into the potential in which particles move.

In FFs with bulk particles and slow dynamics, particle oscillations and the initial relaxation stage $S_{\text{odd}}(t) \sim t$ were observed. The relaxation phenomena in the behavior of the odd component can be completely observed in experiments with polymer solutions. Fast relaxation was observed in the macromolecule on the segment scale (Fig. 7) in agreement with the model $S_{\text{odd}}(t/\tau) \sim t\exp(-t/\tau)$ (Fig. 2) at temperatures $T_1$ = 25.9°C and $T_2$ = 26.2°C (experiment 1 and 2 for a day) (Fig. 8). The even part of the scattering function is described by

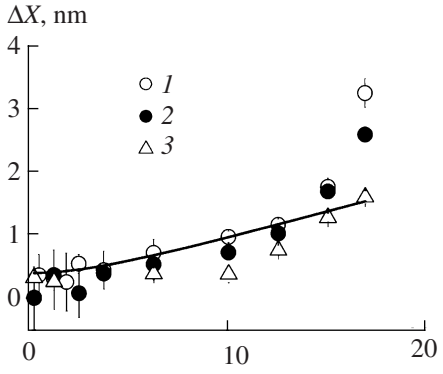


**Fig. 7.** Particle displacements at momenta $q_1$, $q_2$, and $q_3$. The curve is the fitting function $\Delta X = [a^2 + (vt)^2]^{1/2}$ for data *1*.

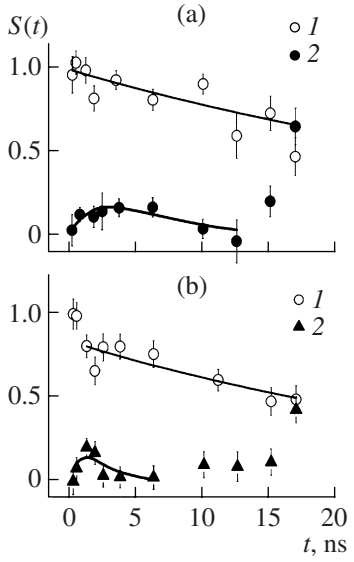


**Fig. 8.** (*1*) Even and (*2*) odd PVCL dynamics at $T_1$ (a) and $T_2$ (b). Curves are fitting functions.

diffusion dependence $S_{even}(t) = S_0\exp(-Dq^2t)$ with the parameters

$$S_{01} = 0.995 \pm 0.049; \quad D_1 = (2.5 \pm 0.8) \times 10^{-6}\ \text{cm}^2/\text{s} \text{ at } T = T_1;$$

$$S_{02} = 0.836 \pm 0.041; \quad D_2 = (3.1 \pm 0.7) \times 10^{-6}\ \text{cm}^2/\text{s} \text{ at } T = T_2.$$

At a small temperature difference, $\Delta T = T_2 - T_1 = 0.3°\text{C}$, the diffusivities are close and yield the hydrodynamic particle diameter $D_H = kT/3\pi\eta \sim 1.6$ nm. At temperatures $T_1 < T_2$, only diffusion is observed. However, at $T_2$, the linear region $\ln[S(t)]$ is preceded by a signal decrease to $S = S_{02} = 0.836$ for a time $t \sim 2$–3 ns, which is associated with odd dynamics. In the first experiment ($T_1$), an $S_{odd}(t)$ maximum in the time interval $t = 0$–12 ns was observed, followed by a rapid increase in $S_{odd}(t)$ at $t > 12$ ns. In the second experiment ($T_2$), a narrow maximum in the time interval $t = 0$–4 ns was detected, followed by a weak signal variation at $t < 15$ ns. The odd spin-echo signal in the region of the maximum is described by the function $S_{odd}(t/\tau) = S_{00}(t/\tau)\exp(-t/\tau)$ with the parameters

$$S_{001} = 0.47 \pm 0.09; \quad \tau_1 = 3.1 \pm 0.5 \text{ ns};$$
$$S_{002} = 0.41 \pm 0.17; \quad \tau_2 = 1.1 \pm 0.3 \text{ ns}.$$

The extraordinary fast process is not directly associated with diffusion at the segment level, since the diffusivity is almost constant in these experiments. The system is far enough from the θ-point ($T_\theta = 32°\text{C}$); therefore, it is difficult to explain a decrease in the relaxation time by a factor of ~3 by a small temperature increase, $\Delta T \sim 0.3°\text{C}$. Undoubtedly, the major role in this process is played by slow structural relaxation processes in a sufficiently concentrated solution, where the polymer concentration $C = 1.4$ g/dl is almost three times larger than the coil overlap threshold $C^* \sim 0.5$ g/dl. Under these conditions, coils are strongly overlapped and mutually penetrate. This retards reaching the equilibrium distribution of units in the volume. As equilibrium is approached, random contacts of coil units disappear and transform to systematic ones. In this case, relaxation is accelerated due to the enhanced interaction of chains, which does appear in the dynamics. The signal $S_{odd} \sim (\omega\tau)/[1 + (\omega\tau)^2]^2$ with a maximum at $\omega_{max} = 1/\tau$ shifts to high frequencies, $\omega_{max1} = 1/\tau_1 \sim 0.3 \times 10^9$ rad/s, $\omega_{max2} \sim 1/\tau_2 \sim 1 \times 10^9$ rad/s.

Odd dynamics can be understood using the resonance models (frequency $\omega_0$, width $\delta$). To a first approximation, the soft mode $S(\omega, \omega_0) = [(\omega - \omega_0)^2 + \delta^2]^{-1}$, where $\omega_0 \sim \delta$ is the sum of even and odd parts $S(\omega, \omega_0) \approx (\omega^2 + \delta^2)^{-1} - 2\omega_0\omega(\omega^2 + \delta^2)^{-2}$, which are corresponded to the spin-echo signals $S_{even}(t\delta) = \exp(-t\delta)$ and $-S_{odd}(t/\tau) = A_\omega(t\delta)\exp(-t\delta)$. Here the parameter $A_\omega = \omega_0/\delta$ under the normalization condition $S_{even}(t = 0) = S_{0even} = 1$, $\delta = 1/\tau$ is related to the relaxation time. From the data of the second experiment, the amplitude parameters $S_{0even} = 1 - S_{02} = 0.16$ and $S_{002} = 0.41$ were obtained, from which it follows that $A_\omega = \omega_0/\delta = S_{002}/S_{0even} = 2.6$ and the frequency $\omega_o = \delta(S_{002}/S_{even}) = 2.3 \times 10^9$ rad/s. The oscillation period $2\pi/\omega_0 \sim 3 \times 10^{-9}$ s at this frequency appears higher than that of torsional oscillations of units ($\sim 10^{-12}$ s) by three orders of magnitude. Hence, the mode characterizes the collective dynamics of the coil ($\sim 10^4$ units), which depends on the solution structure and varies during structural relaxation (Fig. 7).

## CONCLUSIONS

The method for measuring the odd component of the dynamic scattering function which, in combination with the even part, completely describes the dynamics of the system under study was first proposed and experimentally tested.

The results of the study of ferromagnetic fluid and polymer solution first provide insight into the even and odd dynamics of nanosystems, showing the specificity of the phenomena associated with the parity violation of the scattering function.

The new NSE field is interesting with respect to the possibility of studying nonequilibrium states, stochastic dynamics, nonlinear excitations of nanoscopic systems, and many other phenomena which were beyond experimental capabilities.

## ACKNOWLEDGMENTS

This study was supported by the Russian Foundation for Basic Research, project no. 07-03-00074a.

## REFERENCES

1. F. Mezei, Z. Phys. **255**, 146 (1972).
2. *Lecture Notes in Physics, Neutron Spin Echo*, Ed. by F. Mezei (Springer, Berlin, Heidelberg, New York, 1980), vol. 128, p. 3.
3. *Lecture Notes in Physics, Neutron Spin Echo Spectroscopy: Basics, Trends and Application*, Ed. by F. Mezei, C. Pappas, and T. Gutberlet (Springer, Berlin, Heidelberg, New York, 2002), vol. 601, p. 1.
4. B. Farago and F. Mezei, Physica B **136**, 100 (1986).
5. V. T. Lebedev and G. P. Gordeev, Pis'ma Zh. Tekh. Fiz. **11**, 820 (1985) [Sov. Phys. Tech. Phys. Lett. **11**, 340 (1985)].
6. A. I. Okorokov, *Small-angle Scattering of Polarized Neutrons* (Petersb. Nucl. Phys. Inst., St.-Petersburg, 1996) [in Russian].
7. G. M. Drabkin, A. I. Okorokov, and V. V. Runov, Sov. Phys. JETP **25**, 458 (1972).
8. C. Pappas, Gy. Kali, P. Boni, et al., Physica B **276–278**, 162 (2000).
9. C. M. E. Zeyen, in *Lecture Notes in Physics*, Ed. by F. Mezei (Springer, Berlin, Heidelberg, New York, 1980), Vol. 128, p. 151.
10. R. Pynn, in *Lecture Notes in Physics*, Ed. by F. Mezei (Springer, Berlin, Heidelberg, New York, 1980), vol. 128, p. 159.
11. M. Bee, *Quasi-Elastic Neutron Scattering* (Adam Hilger, Bristol, 1988).

12. S. L. Ginzburg and N. E. Savitskaya, in *Proc. of the XXXIII Winter School, Petersburg Nucl. Phys. Inst. on Physics of Condensed Matter* (Gatchina, Russia, 1999), p. 17.
13. A. G. Gukasov, A. I. Okorokov, F. Fuzhara, and O. Sherp, Pis'ma Zh. Eksp. Teor. Fiz. **37**, 432 (1983) [JETP Lett. **37**, 513 (1983)].
14. S. V. Maleev, Usp. Fiz. Nauk **172**, 617 (2002) [Phys. Usp. **45**, 569 (2002)].
15. V. P. Plakhty, J. Kulda, D. Visser, et al., Phys. Rev. Lett. **85**, 3942 (2000).
16. A. Yu. Grosberg and A. R. Khokhlov, *Statistical Physics of Macromolecules* (Nauka, Moscow, 1980) [in Russian].
17. V. T. Lebedev and Gy. Torok, in *Proc. of the 3rd European Conf. Neutron Scattering* (Montpellier, France, 2003), p. 155.
18. V. L. Aksenov, M. V. Avdeev, M. Balasoiu, et al., J. Magn. Magn. Mater. **258–259**, 452 (2003).
19. V. Lebedev, Gy. Torok, L. Cser, W. Treimer, et al., J. Appl. Crystallogr. **36**, 967 (2003).